Construction and Building Materials 77 (2015) 187–196

Contents lists available at ScienceDirect

Construction and Building Materials

journal homepage: www.elsevier.com/locate/conbuildmat

Study of the internal mechanical response of an asphalt mixture by 3-D discrete element modeling

Huan Feng [a,*], Matteo Pettinari [a], Bernhard Hofko [b], Henrik Stang [a]

[a] DTU, Department of Civil Engineering, Brovej 118, Kgs. Lyngby 2800, Denmark
[b] Institute of Transportation – Research Center for Road Engineering, Vienna University of Technology, Gusshausstraße 28/230/3, 1040 Vienna, Austria

HIGHLIGHTS

- The viscoelastic behavior of asphalt mixture was studied by a 3D DEM model.
- Constant set of Burger's parameters calibrated with laboratory test data.
- The ball density may affect the simulation results.
- The internal stresses distribution under dynamic loading have been investigated.

ARTICLE INFO

Article history:
Received 29 August 2014
Received in revised form 11 December 2014
Accepted 12 December 2014

Keywords:
Asphalt mixtures
Viscoelastic
Discrete element method
Micromechanical modeling
Burger's model
Frequency–temperature superposition

ABSTRACT

In this paper the viscoelastic behavior of asphalt mixture was investigated by employing a three-dimensional Discrete Element Method (DEM). The cylinder model was filled with cubic array of spheres with a specified radius, and was considered as a whole mixture with uniform contact properties for all the distinct elements. The dynamic modulus and phase angle from uniaxial complex modulus tests of the asphalt mixtures in the laboratory have been collected. A macro-scale Burger's model was first established and the input parameters of Burger's contact model were calibrated by fitting with the lab test data of the complex modulus of the asphalt mixture. The Burger's contact model parameters are usually calibrated for each frequency. While in this research a constant set of Burger's parameters has been calibrated and used for all the test frequencies, the calibration procedure and the reliability of which have been validated. The dynamic modulus of asphalt mixtures were predicted by conducting Discrete Element simulation under dynamic strain control loading. In order to reduce the calculation time, a method based on frequency–temperature superposition principle has been implemented. The ball density effect on the internal stress distribution of the asphalt mixture model has been studied when using this method. Furthermore, the internal stresses under dynamic loading have been studied. The agreement between the predicted and the laboratory test results of the complex modulus shows the reliability of DEM for capturing the viscoelastic properties of asphalt mixtures.

© 2014 Elsevier Ltd. All rights reserved.

1. Introduction

Asphalt mixture is a complex system that comprises different materials, including mastic, aggregate and air void, in which the mastic phase exhibits viscoelastic behavior in pavement service conditions. One of the most challenging tasks for pavement engineers is a realistic prediction of asphalt pavement performance, which is dependent on the material properties, the environmental and loading conditions. From the material properties point of view, asphalt mixture's individual components and the way they interact with each other play a significant role in the asphalt mixtures performance.

Due to the difficulties and consumption of measuring, experimental testing is not always the most attractive strategy to study asphalt mixture at micro-scale level. While, numerical simulation based on fundamental material mechanics and theories has the advantage of being able to access the impact of individual material component on the performance of asphalt mixture, and is comparatively more convenient and economical to implement. Discrete element method is one type of numerical simulation method which allows the finite displacement and rotation of discrete particles. Especially after combined with Burger's model, Discrete

* Corresponding author.
E-mail addresses: hufe@byg.dtu.dk (H. Feng), matpe@byg.dtu.dk (M. Pettinari), bernhard.hofko@tuwien.ac.at (B. Hofko), hs@byg.dtu.dk (H. Stang).

http://dx.doi.org/10.1016/j.conbuildmat.2014.12.022
0950-0618/© 2014 Elsevier Ltd. All rights reserved.

Element Method (DEM) could be used as an excellent tool to capture the viscoelastic behavior of asphalt mixture. The commercial software Particle Flow Code 3D (PFC^{3D}) developed by Itasca consulting group has been used in this study.

When it comes to simulating asphalt mixtures with DEM, there are mainly two issues that concern pavement researchers: the aggregate shape and different contact models. First, in order to take into account of the aggregate shape effects, different strategies have been developed. Dondi et al. [1] studied the effect of shape and interlocking of grains on the packing characteristics of the aggregate particles in asphalt mix. The aggregate shape effect was considered by using spheres with different diameters. The degree of aggregate contact and interlocking are found to be a function of grain shape and angularity. Liu et al. [2] developed an algorithm, which could randomly generate irregular polyhedron particles to represent the coarse aggregates. One drawback of this method is the big amount of spheres used will significantly increase the calculation time. By using the advanced imaging techniques, Khattak et al. [3] developed a 2D micro-mechanical discrete element model for hot mix asphalt (HMA) mixtures. The specimen was first scanned to obtain a digital image of the cross-sectional area. Then a black and white digital image was generated that would interpret matrix and aggregate phases, respectively. The digital image was processed to establish a numerical logical matrix of the digital image identifying aggregate and matrix pixels. Yu et al. [4] studied the effect of aggregate size distribution and angularity distribution on dynamic modulus using a 3D discrete element method (DEM). Angular particles are generated using an image-based ball-clumping approach which requires significantly reduced number of balls and is capable of capturing the particle shape and angularity effect. The same approach has been adopted by Chen et al. [5]. In Adhikari's study [6], the microstructure of the asphalt concrete specimen was captured by X-ray tomography techniques. The hollow circular images were produced from the layer of cylindrical X-ray computed tomography (X-ray CT) images. The asphalt concrete images were divided into three phases according to a density index: aggregate, sand mastic and air void phases. This approach could be time-consuming and requires large computational resources despite of its accuracy.

Compared to the codes that model continua, PFC^{3D} works at a more basic level: it 'synthesizes' material behavior from the micro-components that make up the material [7]. In DEM simulation, different materials can be distinguished by assigning different interactions between particles, which is usually called contact models. However, it is difficult to choose such properties so that they could represent the real material, which brought the second main issue with DEM modeling. In order to capture the viscoelastic behavior of asphalt mastic, Burger's model has been introduced in DEM simulation. Liu et al. [8] developed a viscoelastic model of asphalt mixtures with the discrete element method. The relationship between the microscale model input and macroscale material properties was derived, and an iterative procedure was developed to fit the dynamic modulus test data of asphalt mastic with Burger's model, in which the Maxwell model stiffness and damping were initialized first and kept constant, and then the Kelvin model's stiffness and damping were calibrated for each frequency. The same way of calibrating Burger's model was also adopted by Chen et al. [9] and Yu et al. [10]. By using Burger's model, Dondi et al. [11] studied the DSR complex shear modulus of asphalt binder using 3D discrete element approach. The model has been proved to be able to predict complex modulus and the phase angle of the studied polymer modified bitumen over a wide range of temperatures and frequencies. You et al. [12] studied asphalt concrete subjected to haversine loading. Viscoelastic parameters for the Burger's model were calibrated from uniaxial dynamic modulus testing results of asphalt sand mastic, while the Discrete Element (DE) prediction was verified by comparing with the experimental testing results of asphalt. Another difficulty related to the contact models is big amount of design parameters, which usually could not be derived directly from lab data. Effort has been devoted to the study of different design parameters by many researchers. For example, Cai et al. [13] studied the effects of the normal to shear contact stiffness ratio on the bulk properties, the parallel bond radius, the number of particles and their positions. Especially, the nine design parameters of Burger's model have been further investigated in his work.

In summary, existing studies provided meaningful insights into understanding and simulating the dynamic properties of asphalt mixtures with DEM. In this paper, a different method has been developed for calibrating the Burger's model: a constant set of Burger's model parameters, which were obtained by fitting the laboratory test data from the whole testing frequency range, has been used for all the frequencies. In addition, when using the time–temperature superposition principle, the ball density effect on the internal stress distribution of the asphalt mixture model has been further investigated.

2. Objectives and scopes

In order to study the viscoelastic behavior of asphalt mixture based on a three-dimensional discrete element model, the research was carried out in two phases. In the first phase, the laboratory tests were performed and complex modulus of asphalt mixtures has been collected. The model was considered as a whole mixture with uniform contact properties for all the distinct elements. Therefore, the input parameters for the Burger's model were calibrated based on the laboratory test results of the whole asphalt mixture, instead of just the mastic phase which provides the viscoelasticity for the asphalt mixture. A constant set of Burger's model was calibrated for all the loading frequencies, which is different compared to the traditional way of calibration where the Burger's model parameters were calibrated for each loading frequency [8–10]. One of the main objectives of this research is to validate the calibration procedure and the reliability of the unique set of Burger's model for different loading frequencies.

In the second phase, the DEM model was assembled and the internal mechanical response of asphalt mixtures has been studied. In order to reduce the calculation time, a method based on frequency–temperature superposition principle developed by Liu et al. [14] has been adopted. The ball density effect has been further investigated when using this method, which is another objective of this research. The dynamic moduli and phase angles of asphalt mixtures were predicted with 3D discrete element simulation under cyclic loading conditions. By comparing the simulation results with those measured in the laboratory, the predictions of the micromechanical model were validated. In addition, the internal stresses under dynamic loading have been studied.

3. Phase 1

3.1. Laboratory tests

The mechanical properties of the asphalt mixture, used for the calibration of the Burger model, were measured in the Vienna University of Technology. The mixture is a Stone Mastic Asphalt with a maximum aggregates dimension of 11 mm (SMA 11). The adopted bitumen was Polymer modified 45/80-65.

The measurements were collected through a Frequency Sweep test in Direct Tension Compression (DTC) configuration [15]. The test was performed in strain control condition. A sinusoidal strain was applied on a cylindrical sample glued on two steel plates

screwed to the loading rig. The amplitude of the applied strain ε_0 was 35με in order to capture the linear viscoelastic response of the studied bituminous mixture. The tests were conducted in a range of frequency between 0.1 and 40 Hz, at the temperatures of −15°, −10°, 0°, 10° and 20 °C. With measured Force (F_0) and strain (ε_0), phase angle (θ), and the Complex Modulus (E^*) were calculated at different studied temperatures and frequencies using the following Eq. (1):

$$E^*(\omega) = \frac{\sigma_0}{\varepsilon_0} e^{i\theta} = E^I + iE^{II} \quad (1)$$

where E^I is the storage modulus (considered as elastic part) and E^{II} is the loss modulus (considered as viscous part).

The obtained values were used to generate the corresponding Master Curve. According to the time temperature superposition principle, the data collected at various temperatures were shifted with respect to time until the curves merge into a single smooth function. The master curve of dynamic modulus as a function of time formed in this manner describes the loading time dependency of the asphalt mixture. Fig. 1 shows the Master Curve of the studied mixture at the reference temperature of 10 °C, which is representative of the average annual asphalt temperature in Denmark. In particular the values in the range of frequency from 1 to 20 Hz, highlighted in the Fig. 1, have been considered for the Burger parameters calibration.

The adopted range of frequencies can be explained and justified through two different but fundamental reasons. The first is related with the properties of the Burgers model itself. In fact Nilsson et al. [16] shown that Burger's model is a simple one capable of characterizing the viscoelastic property of the asphalt concrete, but it cannot be used for a wide range of frequencies or temperatures. It has been observed that Stiffness Modulus is satisfactory described by Burger model between 0.5 and 40 Hz. Outside of this range the Modulus is underestimated. The corresponding phase angle values are satisfactory fitted only between 5 and 25 Hz. Considering both Stiffness Modulus and Phase angle, the authors shown that Burgers model is able to describe these mechanical properties acceptably over a limited frequency range (in the order of 1–20 Hz).

The second relevant aspect to highlight is related to the need of investigating asphalt mixture response at the natural frequency of a flexible pavement when subjected to traffic loading. As suggested by different authors, the natural frequency, which depends on type and speed of the vehicle as well as temperature and type of pavement structure, can range from 6 to 12 Hz [17,18]. It has been found also that truck loading frequency is about 4.6 Hz at a speed of 58 km/h and 6.5 Hz at 82 km/h [19].

3.2. Calibrations of Burger's model

The contact model describes the constitutive behavior of a contact associated by two particles, playing a significant role in defining DEM modeling. There are two standard contact models (Linear and Hertz) and several alternative contact models including the Burger's model available in PFC^{3D}, the commercial DEM program used in this study. In order to build the constitutive model, four contact models were employed in the asphalt mixture composite, including the slip model, linear stiffness-contact model, contact bond model and Burger's contact model. The stiffness model provides an elastic relation between the contact force and relative displacement. The slip model enforces a relation between shear and normal contact forces such that the two contacting balls may slip relative to one another. The total normal and shear forces that the contact can carry could be defined in the bonding model by enforcing bond-strength limits.

The Burger's model is comprised of a Kelvin model and a Maxwell model connected in series in both the normal and shear directions, which is able to provide the considerations of the time dependent characteristic of asphalt mixture in a relative effective and simple way. Burger's model has four parameters, but as both normal and shear directions have to be considered, eight parameters need to be included to describe the contact relations between two microscopic particles, as listed in Table 1. Furthermore, friction coefficient (f_s) between balls in the DEM model should be considered when slip between balls occurs.

Table 1
Denotations of Burger's model parameters.

	Normal stiffness	Normal viscosity	Shear stiffness	Shear viscosity
Kelvin	K_{kn}	C_{kn}	K_{ks}	C_{ks}
Maxwell	K_{mn}	C_{mn}	K_{ms}	C_{ms}

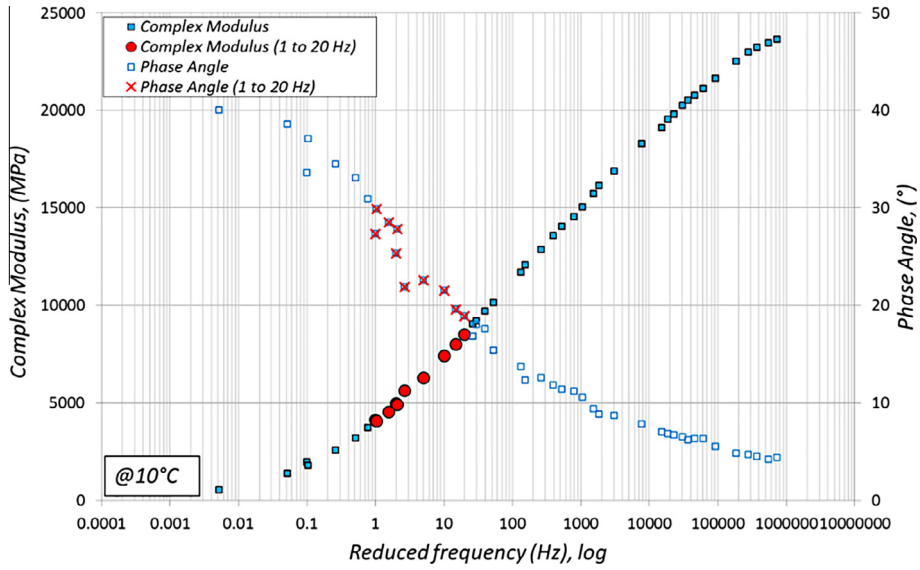

Fig. 1. Master curve of SMA 11 at +10 °C.

However, when it comes to the calibration of model parameters, one of the challenges is that there is no direct link between those values and the experimental results, due to the fact that they are related to the micromechanical properties of the material. Therefore, a macroscale Burger's model will first be established to be correlated to the experimental dynamic modulus and phase angle, as shown in Fig. 2. The parameters of the macroscopic Burger's model can then be converted into the microscopic model parameters.

Total strain in the Burger's model may be written as:

$$\varepsilon = \varepsilon_{de} + \varepsilon_{ie} + \varepsilon_{cp} \tag{2}$$

where, ε_{de}, ε_{ie} and ε_{cp} = elastic strain, viscous strain and delayed elastic strain. Further, stress–strain relationship may be written as:

$$\sigma = E_1\varepsilon_{ie} \qquad \sigma = \eta_1\frac{\partial}{\partial t}\varepsilon_{cp} \qquad \sigma = E_2\varepsilon_{de} + \eta_2\frac{\partial}{\partial t}\varepsilon_{de} \tag{3}$$

substituting Eq. (3) into Eq. (2), we could obtain:

$$\varepsilon = \frac{\sigma}{E_1} + \frac{\int \sigma dt + C_1}{\eta_1} + e^{\int -\frac{E_2}{\eta_2 dt}}\left(\int \frac{\sigma}{\eta_2} e^{\int \frac{E_2}{\eta_2 dt}} dt + C_2\right) \tag{4}$$

where E_1, η_1, η_2 and E_2 = Burger's model parameters as mentioned σ and ε = stress and strain; C_1 and C_2 = constants determined by the following equations when $t = 0$ [20].

$$\frac{\int \sigma dt + C_1}{\eta^1} = 0 \qquad e^{\int -\frac{E_2}{\eta_2 dt}}\left(\int \frac{\sigma}{\eta_2} e^{\int \frac{E_2}{\eta_2 dt}} dt + C_2\right) = 0 \tag{5}$$

When asphalt mixtures are subjected to dynamic stress $\sigma^* = \sigma_0 e^{i\omega t}$, the resulting dynamic strain is described as $\varepsilon = \varepsilon^* e^{i\omega t}$ [21].

The axial complex modulus is defined as the complex quantity:

$$\frac{\sigma^*}{\varepsilon^*} = E^*(i\omega) = \left(\frac{\sigma_0}{\varepsilon_0}\right)e^{i\varphi} = E_1 + iE_2 \tag{6}$$

in which σ_0 is the stress amplitude, ε_0 is strain amplitude, and ω is angular velocity, which is related to the frequency by $\omega = 2\pi f$. The ratio of the stress and strain amplitudes σ_0/ε_0 define the dynamic modulus $|E^*(\omega)|$, shown in Eq. (7).

$$|E^*(\omega)| = \sqrt{E_1^2 + E_2^2} = \frac{\sigma_0}{\varepsilon_0} \tag{7}$$

Consequently, the complex compliance, which is the reciprocals of the dynamic modulus, can be expressed using the following equation:

$$D^*(\omega) = \frac{\varepsilon^*}{\sigma_0} = \frac{1}{K_m} + \frac{1}{i\omega C_m} + \frac{1}{K_m + i\omega C_k} \tag{8}$$

where, σ and ε^* are the stress and strain at time equals zero, ω is the radial frequency, and t is the elapsed time. The complex compliance consists of real portion and imaginary portion, and is normally written as:

$$D^*(\omega) = D'(\omega) + iD''(\omega) \tag{9}$$

$$D'(\omega) = \frac{1}{K_m} + \frac{K_k}{K_k^2 + \omega^2 C_k^2} \tag{10}$$

$$D''(\omega) = \frac{1}{\omega C_m} + \frac{\omega C_k}{K_k^2 + \omega^2 C_k^2} \tag{11}$$

The dynamic compliance is determined as $|D^*| = \sqrt{(D')^2 + (D'')^2}$. And the dynamic modulus is the reciprocals of the complex compliance, that is:

$$|E^*| = \frac{1}{|D^*|} = \frac{1}{\sqrt{(D')^2 + (D'')^2}} = \frac{1}{\sqrt{\left(\frac{1}{K_m} + \frac{K_m}{K_k^2+\omega^2C_k^2}\right)^2 + \left(\frac{1}{\omega C_m} + \frac{\omega C_k}{K_k^2+\omega^2C_k^2}\right)^2}} \tag{12}$$

The phase angle φ can be expressed as:

$$\varphi = tan^{-1}\left(\frac{D''}{D'}\right) = tan^{-1}\left(\frac{K_m}{\omega C_m}\frac{K_k^2 + \omega^2C_k^2 + \omega^2C_kC_m}{K_k^2 + \omega^2C_k^2 + K_kK_m}\right) \tag{13}$$

Eqs. (2)–(13) describe the equations for determining the macroscale parameters of asphalt mixtures. Once the macroscale parameters are obtained, the microscale parameters can be obtained from the following equations:

$$K_{mn} = K_mL, \quad C_{mn} = C_mL \tag{14}$$

$$K_{kn} = K_kL, \quad C_{kn} = C_kL \tag{15}$$

where, $L = R(A) + R(B)$, which is the sum of the radius of two contact balls A and B.

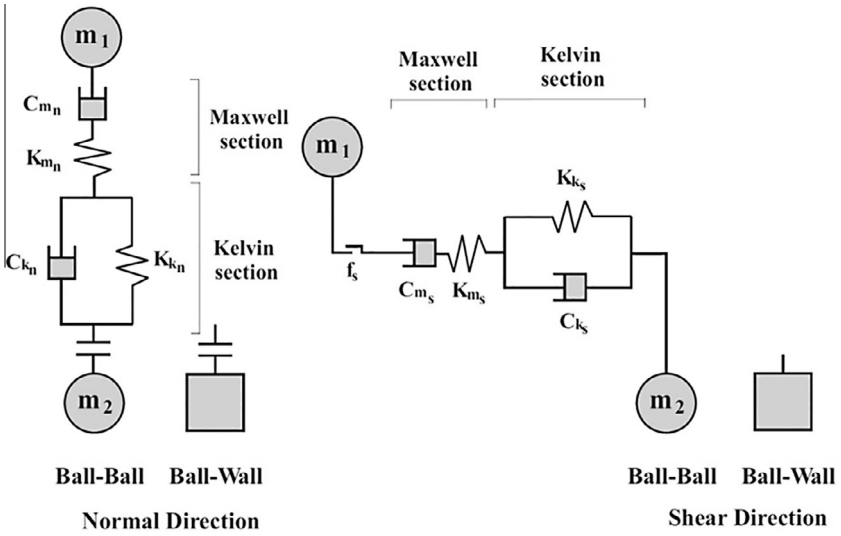

Fig. 2. Macroscale mechanical entities of Burger's model.

Table 2
Complex modulus from experimental testing at 10 °C.

f [Hz]	1	5	10	15	20
E^* [GPa]	4.12	6.28	7.4	8.02	8.49
φ [°]	27.3	22.6	21.5	19.6	18.9

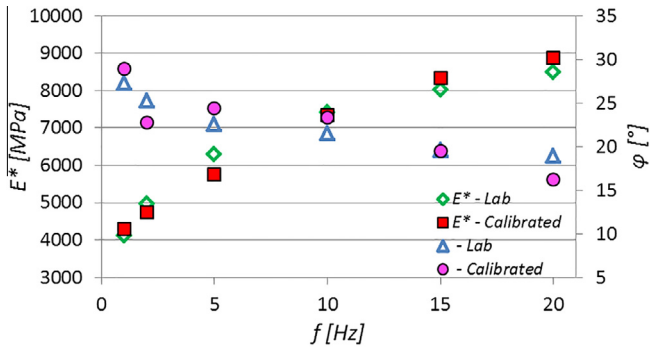

Fig. 3. Calibration for input parameters of Burger's contact model fitted with lab test data.

Table 3
Calibrated Burger's model parameters.

K_k [MPa]	K_m [MPa]	C_k [MPa · s]	C_m [MPa · s]
12.78	13.47	0.38	2.31

3.3. Frequency–temperature superposition

In order to reduce the computation time for discrete-element (DE) model of asphalt-based materials, the methodology developed by Liu et al. [14] was adopted, which is based on the frequency–temperature superposition principle. According to this principle, the behaviors of a time dependent material are dependent on temperatures and loading frequencies. The effects of temperatures and frequencies can be equivalently and mathematically expressed as:

$$E(\omega_1, T_1) = E(\omega_2, T_2) \tag{16}$$

where, E = time-dependent property, such as dynamic modulus and phase angle; ω_1 and T_1 = angular frequency and the loading temperature in the laboratory test; and ω_2 and T_2 = reduced angular frequency at the reference temperature and the reference temperature, respectively.

Instead of being directly involved in the calculation of shifting factor, the temperatures T_1 and T_2 were used to modify the Burger's model parameters. In Burger's model, only the viscosities of the two dashpots can represent the effects of temperatures or loading frequencies due to the fact the spring elements are independent of time and temperatures. Therefore, the frequency–temperature superposition in Eq. (16) could be presented as:

$$E(\omega_1, \eta_m(T_1), \eta_k(T_1)) = E(\omega_2, \eta_m(T_2), \eta_k(T_2)) \tag{17}$$

where, $\eta_m(T_1)$ and $\eta_k(T_1)$ represent the time-dependent properties at T_1, whereas $\eta_m(T_2)$ and $\eta_k(T_2)$ represent the time-dependent properties at T_2. Based on Liu's study [14], a time-dependent material property, such as complex modulus in this case, can be equivalently expressed with the Burger's model parameters at the amplified frequency $\omega_2 = \xi\omega_1$, as long as the viscosities of the two dashpots in the Burger's model are also amplified correspondingly, as shown below in Eqs. (18)and (19):

$$\eta_M(T_2) = \frac{\omega_1}{\omega_2}\eta_M(T_1) = \frac{\eta_M(T_1)}{\xi} \tag{18}$$

$$\eta_K(T_2) = \frac{\omega_1}{\omega_2}\eta_K(T_1) = \frac{\eta_K(T_1)}{\xi} \tag{19}$$

Because the virtual frequencies were much larger than the regular frequencies, the computation time was significantly reduced by conducting the DE modeling with the virtual frequencies and the corresponding modified Burger's parameters. In this study, the loading frequencies were amplified by 1000 (ξ = 1000).

3.4. Results of Burger's model calibrations

The dynamic modulus and phase angles measured from the lab tests are shown in Table 2. A constant set of Burger's contact model parameters were calibrated by fitting the lab test results from the whole frequency range using the equations derived above. A good agreement between the fitting and measured dynamic modulus and phase angle were obtained, as shown in Fig. 3. The Parameters for Burger's contact model are listed in Table 3. Due to the fact that only the stresses in normal direction were measured in the lab so the same parameters have been used for both the normal and shear direction in the simulation.

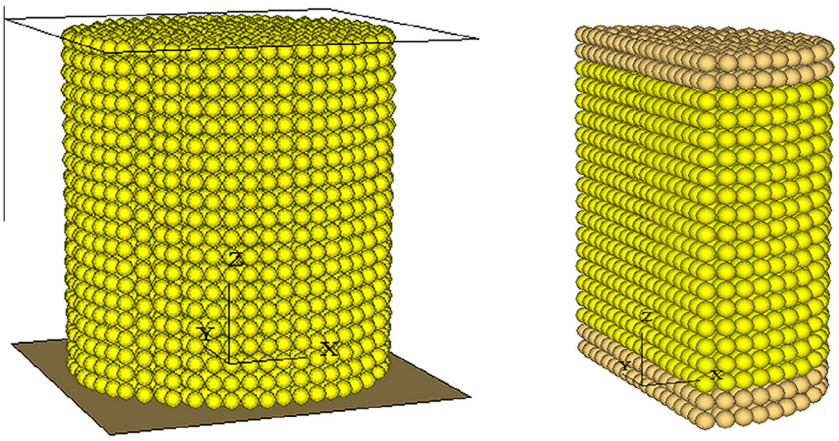

Fig. 4. Discrete element model in *PFC*^{3D}.

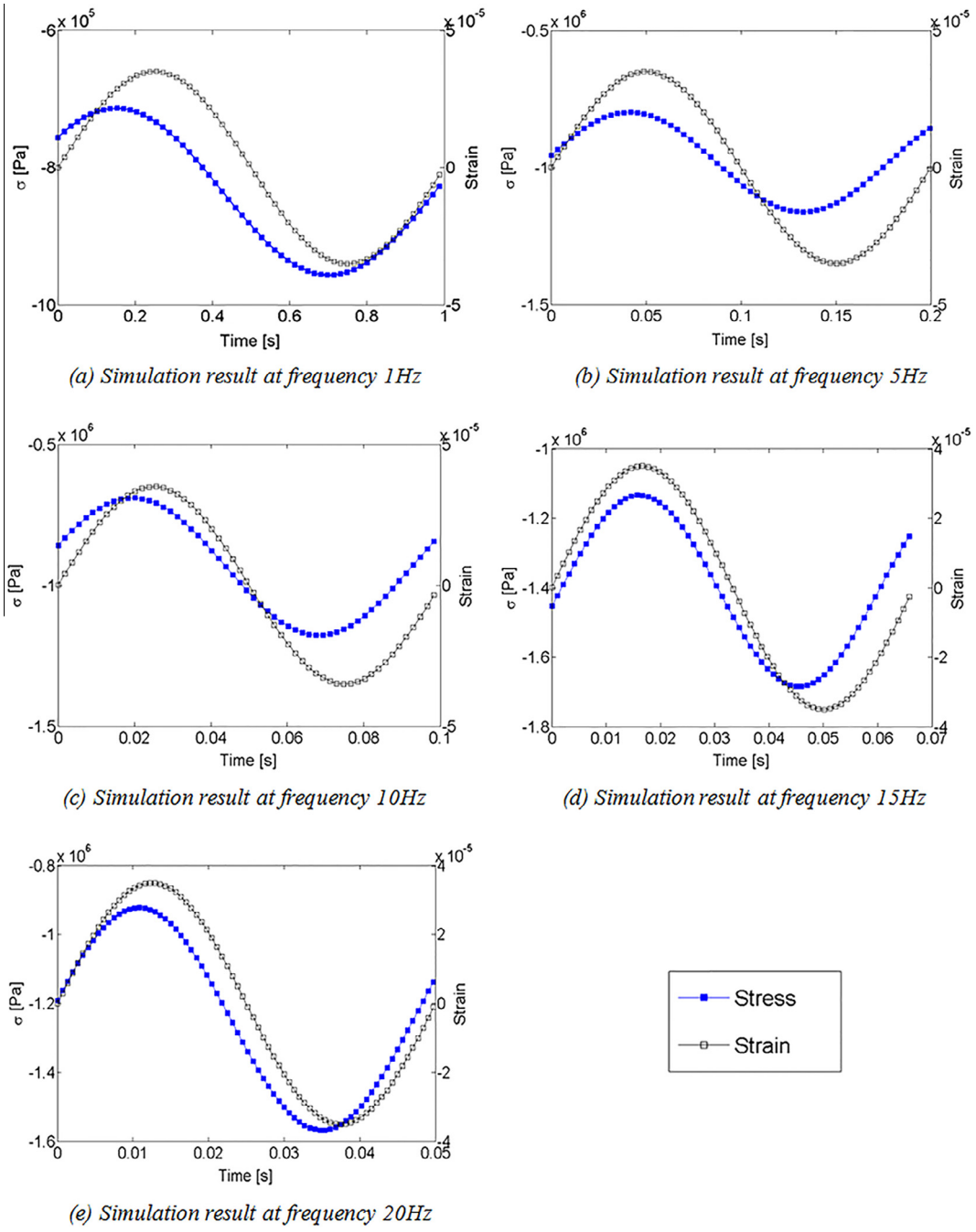

(a) Simulation result at frequency 1Hz

(b) Simulation result at frequency 5Hz

(c) Simulation result at frequency 10Hz

(d) Simulation result at frequency 15Hz

(e) Simulation result at frequency 20Hz

Fig. 5. Applied strain and corresponding stress in DEM simulation.

4. Phase 2: Numerical analysis

4.1. Internal mechanical response

4.1.1. DEM simulation of the complex modulus

In this research study, the model parameters for DE simulation were determined using the procedure discussed previously in this paper. Experimental testing results at the same temperature and frequencies were used to calibrate the DEM models. The viscoelastic DE simulation was conducted with the corresponding model parameters under the cyclic uniaxial compression loadings. As shown in Fig. 4, the cylindrical model is 2 cm in height and 2 cm in diameter, which comprises 5860 spheres. Compressive dynamic loads in the z-direction were applied to the top loading plate of the digital sample, while the bottom plate of this sample was fixed in all directions. The applied load frequencies were 20, 15, 10, 5 and 1 Hz. The motions of the spheres on top and bottom layers were slaved to the motions of the loading plates in order to simulate the glue effect in the laboratory. Prior to the actual simulation, the sample was compacted in order to achieve an initial isotropic stress state.

The applied strain and stress response are plotted in Fig. 5 for each loading frequency. The average stress of the model was measured by measure spheres installed. Dynamic modulus (E^*) and

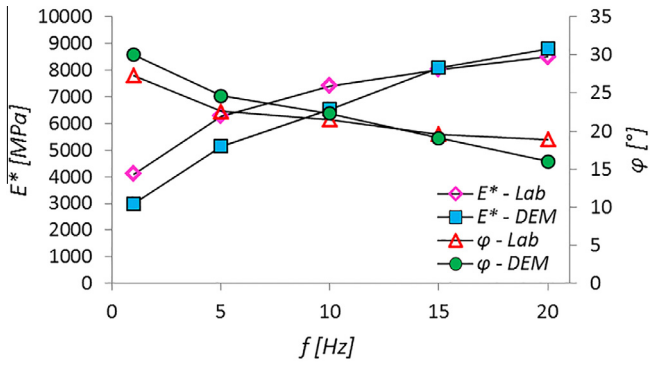

Fig. 6. Comparison of the predicted and measured dynamic modulus and phase angles.

phase angle (φ) were calculated from the stress and strain curve in Fig. 5 using Eq. (20). The predicted E^* and φ are plotted in Fig. 4 along with those measured in the laboratory.

$$E^* = \frac{\sigma_{max} - \sigma_{min}}{\varepsilon_{max} - \varepsilon_{min}} \qquad \varphi = \frac{\Delta t}{\tau} \times 360 \tag{20}$$

where, ε_{max}, ε_{min}, σ_{max} and σ_{min} = maximum and minimum values of the applied strain and the calculated stress response; Δt = time difference between two adjacent peak strains; and T = loading period, which is the inverse of the loading frequency.

4.1.2. Predictions results of complex modulus

Fig. 6 compares the predicted dynamic modulus and phase angles from DEM simulation with the laboratory test results. As we can see from the results, the dynamic modulus from DE viscoelastic models were generally slightly under-predicted, while the predicted phase angles were slightly higher compared with the experimental values. The average prediction error for phase angle is only 0.97%. The predicted dynamic modulus has an average prediction error of 8.53%. Possible reason for this error could be related to the simplicity of the model, in which only the material property in normal direction was calibrated from the laboratory results. The favorable agreement between the discrete element prediction and the lab results on dynamic modulus and phase angles indicates that the viscoelastic discrete element model developed in this study has the ability to predict the complex viscoelastic properties of asphalt mixtures with the confidence of more than 90%.

4.1.3. Internal stress distribution and velocities of balls

In order to study the internal mechanical responses of the sample under dynamic loading, measure spheres have been used. Five positions along the height of the sample were picked up, and at each height five measure spheres were installed, as shown in Fig. 7. The stress at each height was calculated as the average stress of those measured from the five measure spheres. Furthermore, the relative velocities Δv in loading direction z between the top and bottom spheres inside each measure sphere have been monitored.

Eight time points were picked up during one loading cycle, as shown in Fig. 8. Together with the sphere velocity vectors, internal stresses response and the relative sphere velocities along the height of the DE viscoelastic model were demonstrated in Fig. 9. Obviously the internal stresses are not homogenous for viscoelastic model compared with elastic model. The axial stresses on the top part of the sample always have higher amplitude than the lower part. The response of the sphere velocity vectors might help with achieving better understanding of this phenomenon. The velocity of each ball is drawn as an arrow, with length proportional to magnitude, and orientation equal to that of the velocity vector. Besides the obvious contractions and expansions in the middle part of the sample, it is clear that mainly the upper half of the model is affected by the motion of the top loading plate. The relative velocities in loading direction between the nearby up and down spheres are decreasing from the top to the bottom of the sample, which shares similar pattern with the internal stress responses. As shown in Figs. 8 and 9, when the absolute values of the relative sphere

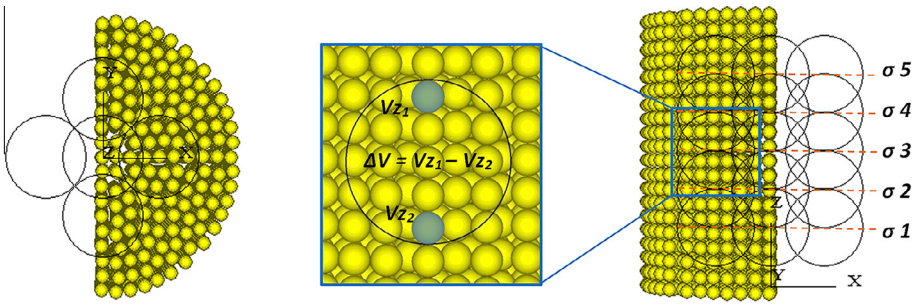

Fig. 7. Measure spheres installed in the model.

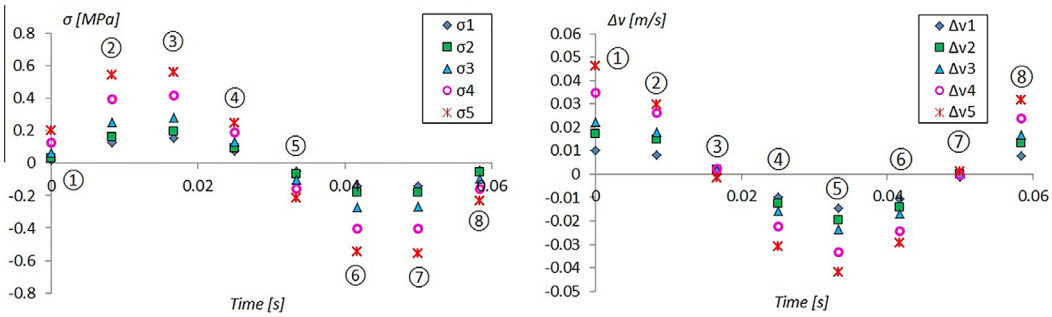

Fig. 8. Internal stresses and relative sphere velocities along the height of the sample during one loading cycle.

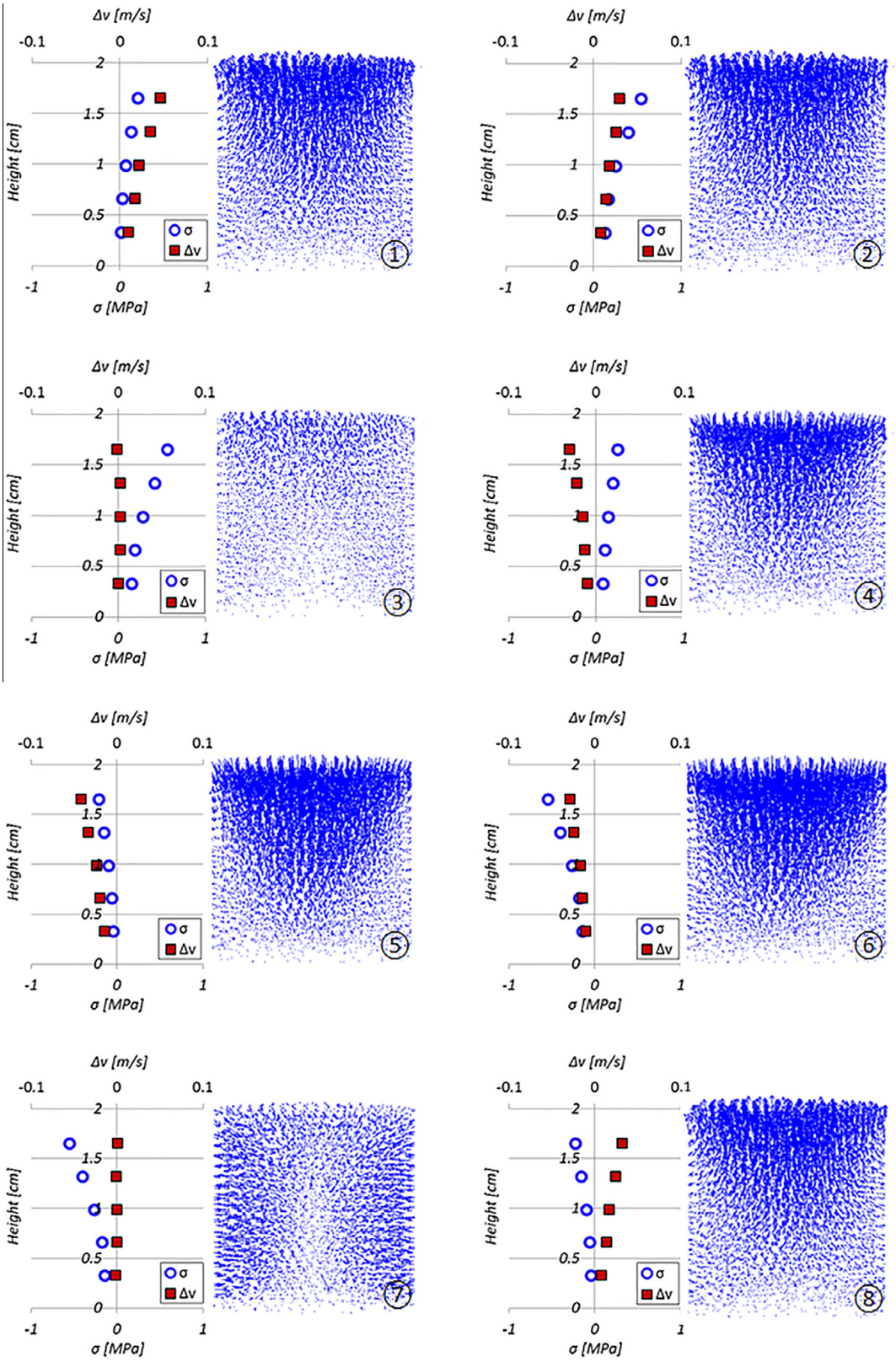

Fig. 9. Internal stresses, relative sphere velocities along the height and sphere velocity vectors during one loading cycle.

velocities become zero (time point 3 and 7), the internal stresses achieve their maximum; whereas when the absolute value of the relative sphere velocities reaches their maximum (time point 1 and 5), the values for internal stresses are around zero. *PFC*^{3D} is based on repeated application of law of motion to each particle, and force–displacement law to each contact. From this point of view, bigger relative velocities between contiguous spheres will certainly result in larger relative displacements within accumulated time, which eventually will lead to the decreasing trend of strains and stresses from the top to the bottom of the sample. This

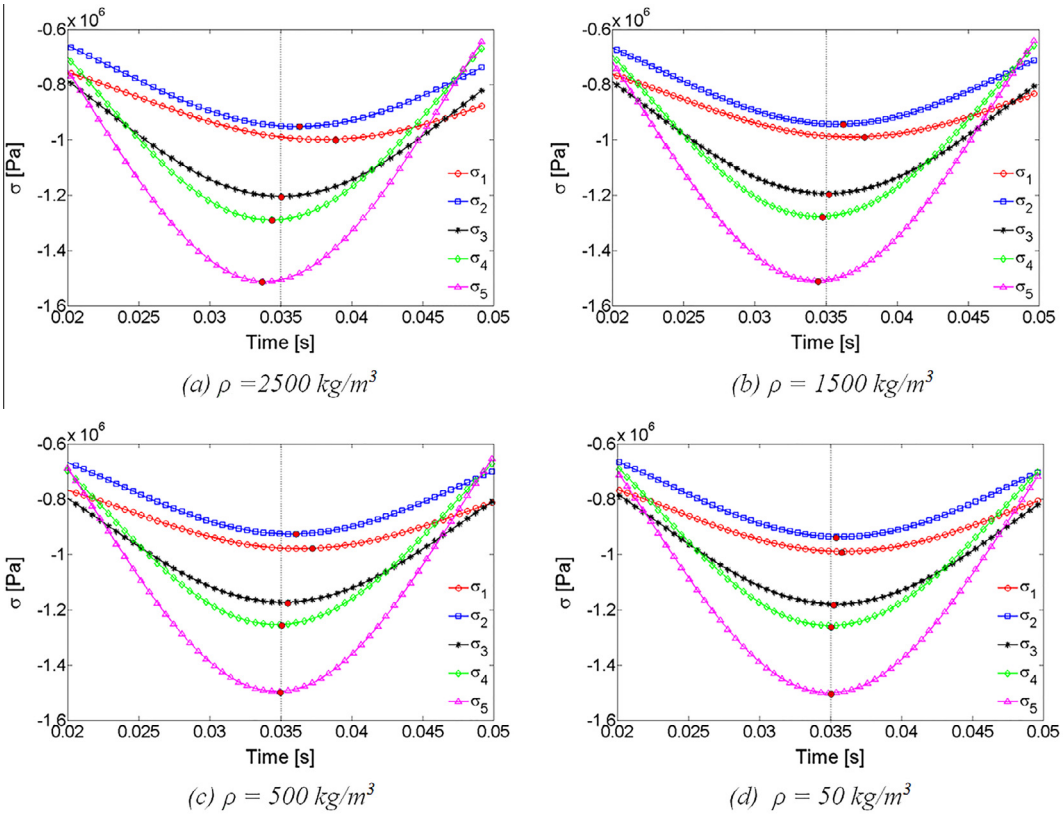

Fig. 10. Stresses at different heights of the asphalt mixture model with different ball densities ρ at 20 Hz.

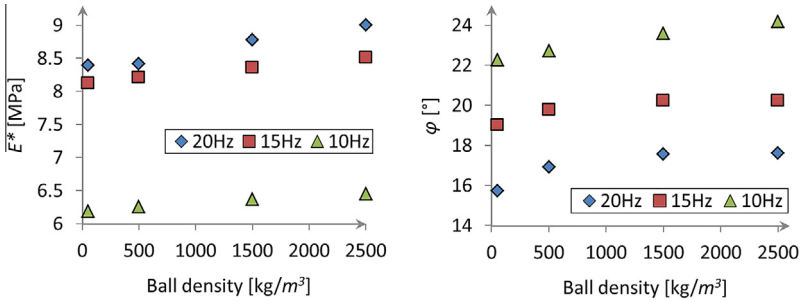

Fig. 11. Sphere density effect on dynamic modulus E^* and phase angle φ.

result could also be used as an explanation for laboratory observations obtained from a tension and compression fatigue test of asphalt mixtures, in which most of the time the failure occurs at the top part of the sample when fatigue characterization is completed. This could also lead to the conclusion that under dynamic loading conditions higher energy is dissipated on the top part of the asphalt mixtures sample.

4.2. Effect of sphere's density

It has been observed that when using the time–temperature superposition principle, the density of the balls has a significant effect on the internal stress distribution of the asphalt mixture model. Fig. 10 shows the internal stress distribution of the asphalt mixture model during dynamic compression with different ball density, from 2500 kg/m^3 reduced to 50 kg/m^3. Obviously, the smaller the sphere density is, the better consistency relative to time could be obtained for stresses at different positions along the height. For example, when the ball density is 2500 kg/m^3, stresses at different height have their peaks at different time point. While when the density is 50 kg/m^3, stresses from all the locations achieved their peak at the same time point 0.035 s. The reason for this is when applied loading frequencies are so highly amplified that the effect of the mass inertia will be amplified at the same time. Therefore, lower densities should be used in the simulations. Furthermore, increasing the ball density will cause a bigger predicted dynamic modulus and phase angle. As shown in Fig. 11, the ball density effect on dynamic modulus and phase angle is almost linear. However, significant sphere density reduction will also prolong calculation time. Eventually, density 50 kg/m^3 has been used in this study, which could offer both a reasonable stress consistency and an affordable calculation time at the same time.

5. Summary and conclusion

This paper developed a micromechanical discrete element modeling method to simulate the complex modulus properties of asphalt mixtures based on a viscoelastic Burger's contact model.

The microscale input parameters of the DE model were determined by the corresponding lab-based macroscale material properties. Viscoelastic DE simulation with developed model was conducted under uniaxial compression loading with different loading frequencies. The dynamic modulus and phase angles were calculated and compared with those measured in the laboratory. In order to overcome the time-consuming limitation of DEM calculation, the frequency–temperature superposition principle has been adopted. The normal loading frequencies in the laboratory tests were amplified, and the fitted Burger's contact model parameters were converted into those at the amplified frequencies. The sphere density effect has been studied when using this principle. The following findings were observed:

1. The dynamic modulus from DE viscoelastic models was generally slightly under-predicted, while the predicted phase angles were slightly higher compared with the experimental values. Possible reason for the error could be related to the simplicity of the model, in which the shear properties of the material was not considered. The favorable agreement between the 3D DEM prediction and the laboratory measurements indicates that 3D discrete element model developed in this study is capable of capturing the viscoelastic properties of asphalt mixtures.
2. Under the dynamic loading, the internal stresses observed from this viscoelastic model are not homogenous compared to other elastic models. The stresses on the top part of the sample always have higher amplitudes than the lower part. Explanations might be found in the responses of sphere velocity: besides the obvious contractions and expansions in the middle part of the sample in the velocity vector plot, it is clear that mainly the upper half of the model is affected by the motion of the top loading plate. In addition, the relative sphere velocities in the loading direction share similar pattern with the internal stress, which is decreasing from the top to the bottom. Considering the fact that PFC^{3D} is based on repeated application of law of motion to each particle, and force–displacement law to each contact, it is reasonable that higher relative sphere velocities will cause larger displacements within accumulated time, and consequently the uneven strains distribution along the sample height. This could be the reason why the stresses on the upper half of the sample are higher than the lower part. The laboratory observations obtained from a tension and compression fatigue test of asphalt mixtures coincides with this result, in which most of the time the failure occurs at the top part of the sample. This also means under dynamic loading conditions higher energy is dissipated on the top part of the asphalt mixtures sample.
3. By using a method based on the frequency–temperature superposition principle, less calculation time is needed for the 3D viscoelastic DE simulation of asphalt mixtures. On the other hand, when using this method the sphere density plays a significant role in the internal stress distribution of the asphalt mixture model. The reason for this is because the amplified frequencies will increase the effect of the ball mass inertia at the same time. In order to minimize the ball mass effect, the density used in the simulation should be as low as possible. However, due to the fact that smaller ball density would result in longer calculation time. Therefore, a relatively low density has been used in this study, which could offer a reasonable stress consistency and affordable calculation time at the same time.

The current model is able to capture the viscoelastic properties of asphalt mixtures at the real traffic loading frequencies, with the advantage of conveniently providing the internal mechanical response of the material at macro-scale inside the flexible pavement structure. Furthermore, a feasible way to study the correlation between the amounts dissipated energy and the rolling resistance of asphalt mixtures could also be obtained through the developed DEM model.

Acknowledgement

The authors gratefully acknowledge the funding support by the COOEE Project.

References

[1] Dondi G, Simone A, Vignali V, Manganelli G. Discrete particle element analysis of aggregate interaction in granular mixes for asphalt: combined DEM and experimental study. In: 7th RILEM international conference on cracking in pavements. RILEM book series, vol. 4; 2012. p. 389–98.
[2] Liu Y, You Z. Visualization and simulation of asphalt concrete with randomly generated three dimensional model. J Comput Civil Eng 2009;23(6):340–7.
[3] Khattak MJ, Khattab A, Rizvi HR, Das S, Bhuyan MR. Imaged-based discrete element modeling of hot mix asphalt mixtures. Mater Struct 2014. http://dx.doi.org/10.1617/s11527-014-0328-1.
[4] Yu H, Shen S. Impact of aggregate packing on dynamic modulus of hot mix asphalt mixtures using three-dimensional discrete element method. Constr Build Mater 2012;26(1):302–9.
[5] Chen J, Pan T, et al. Predicting the dynamic behavior of asphalt concrete using 3D DEM. J Wuhan Uni Technol Mater Sci April 2012;27(2):382–8.
[6] Adhikari S, You Z. 3D discrete element models of the hollow cylindrical asphalt concrete specimens subject to the internal pressure. Int J Pavement Eng 2010;11(5):429–39.
[7] Itasca consulting group, Inc. PFC 3D Ver. 4.0, Minneapolis; 2008.
[8] Liu Y, Dai Q, You Z. Viscoelastic model for discrete element simulation of asphalt mixtures. J Eng Mech 2009;135(4):324–33.
[9] Chen J, Pan T, Huang X. Discrete element modeling of asphalt concrete cracking using a user-defined three-dimensional micromechanical approach. J Wuhan Uni Technol Mater Sci Ed December 2011;26(6):1215–21.
[10] Yu H, Shen S. A micromechanical based three-dimensional DEM approach to characterize the complex modulus of asphalt mixtures. Constr Build Mater 2013;38:1089–96.
[11] Dondi G, Vignali V, Pettinari M, Mazzotta F, Simone A, Sangiorgi C. Modeling the DSR complex shear modulus of asphalt binder using 3D discrete element approach. Constr Build Mater 2014;54:236–46.
[12] You Z, Liu Y. Three-dimensional discrete element simulation of asphalt concrete subjected to haversine loading. Road Mater Pavement Des 2010;11(2):273–90.
[13] Cai W, McDowell GR, Airey GD. Discrete element visco-elastic modelling of a realistic graded asphalt mixture. Soils Found 2014;54(1):12–22.
[14] Liu Y, You Z. Accelerated discrete-element modeling of asphalt-based material with frequency–temperature superposition principle. J Eng Mech 2011;137(5):355–65.
[15] EN 12697-26, Bituminous mixtures – test methods for hot mix asphalt – Stiffness; 2012.
[16] Nillson RN, Hopman PC, Isacsson U. Influence of different rheological models on predicted pavement responses in flexible pavements. Road Mat Pavement Des 2002;3(2):117–49.
[17] Uddin W. Effects of FWD Load-Time History on Dynamic Response Analysis of Asphalt Pavement, Pavement Performance Data Analysis Forum in Conjunction with MAIREPAV03, Guimaraes, Portugal, 2003.
[18] Darestani M Y, David P T, Andreas N, Daksh B. Dynamic response of concrete pavements under vehicular loads. In: Proc., IABSE symposium—response to tomorrow's challenges in structural engineering, Budapest, Hungary; 2006. p. 104–5.
[19] Gillespie TD, Karimihas SM, Cebon D, Sayers MW, Nasim MA, Hansen W, et al. NCHRP Report 353: effects of heavy vehicle characteristics on pavement response and performance. Washington, DC: TRB, National Research Council; 1993.
[20] Maina J W, Anochie-Boateng J, Matsui K Application of visco-elastic model to flexible pavement analysis. In: 10th Conference on Asphalt Pavements for Southern Africa; 2011.
[21] Kim YR. Modeling of Asphalt Concrete. ASCE Press; 2009.